[From MEMOIRS of the School of Science & Engineering. No. 54 (1990) pp. 1～22]

Analyses of Bending Moments and Shearing Forces in Flat Slab Construction

By

GENGO MATSUI

WASEDA UNIVERSITY

MEMOIRS OF THE SCHOOL OF
SCIENCE & ENGINEERING
WASEDA UNIV., NO. 54, 1990

Analyses of Bending Moments and Shearing Forces in Flat Slab Construction

GENGO MATSUI*

This paper discusses two analyses in flat slab construction; one is for column arrangements and the other is for shapes of drop panel.

The solutions are derived from the analogy between the bending moments of a plate and the deflection of a membrane.

Membrane experiments are conducted by the Moire Method.

Through the analysis regarding column arraugements, it is found that a triangular arrangement is the most advantageous, while a hexagonal arrangement is the least advantageous. From the analysis concerning the shapes of the drop panels, the largest shearing forces around the drop panel are found at the edge of a square panel.

It is concluded that these methods are of wide application.

§1. COLUMN ARRANGEMENTS IN FLAT SLAB CONSTRUCTION

In this section, we discuss the most advantageous layout of column arrangement in buildings with regular patterns of column arrangement such as warehouses, garages, supermarkets, etc., and are also concerned with a random arrangement.[1)]

In flat slab construction, columns produce a quasi-frame cooperating with column-strip as a beam, but it doesn't have enough stiffness for earthquake load. Since horizontal loads are generally supported by the external walls or shear walls of the building, the quasi-frame for a flat slab construction is regarded as supporting only uniformly distributed vertical floor load.

In general, slabs are subjected to both bending and torsional moments. Since the tortional moments are held by concrete, the amount of reinforcement is depend on the bending monents. As slab has enough thickness in flat slab construction, it is usually under a balanced steel ratio, and hence the amount of reinforcing bars is considered to be proportional to the bending moments.

In the vicinity of the column head and the middle portion of the slab, the bending moment has the same sign in all directions. Thus sum of the bending moments in any two perpendicular direction indicates the required amount of reinforcing bars.

This paper was solicited by the Editorial Committee in honor of the Author's retirement from Waseda University.

Received Sep. 18, 1990

* Department of Architecture.

The sum of the bending moments is provied as a second order differential equation. Then we consider several sorts of cases for column arrangements. At the center of the column strip, the bending moment has different signs in two perpendicular directions; and the finite element solutions are discussed.

We can realize the analogical relationship between the sum of bending moments and the deflection of a membrane. Based on this analogy we conduct membrane experiments and obtain contour lines by the Moire method.

As for regular patterns of column arrangement, we consider those cases shown in Fig. 1. The load tributary area of each column is marked by a dotted line. These areas are hexagonal for a triangular pattern, square for a rectangular pattern and triangle for a hexagonal pattern.

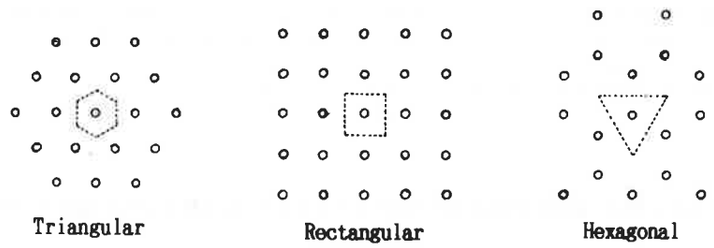

Fig. 1 Column arrangements for flat slab

1.1 The Sum of Bending Moments of a Plate

Taking the x and y axes parallel to a plate, the bending moments M_x, M_y are[2)]

$$M_x = -D\left(\frac{\partial^2 w}{\partial x^2} + \nu\frac{\partial^2 w}{\partial y^2}\right)$$

$$M_y = -D\left(\frac{\partial^2 w}{\partial y^2} + \nu\frac{\partial^2 w}{\partial x^2}\right)$$

in which

D: rigidity of the plate
w: deflection of the plate
ν: Poisson's ratio.

Denoting the sum of these perpendicular bending moments as M, we have

$$M = M_x + M_y = -D(1+\nu)\left(\frac{\partial^2 w}{\partial x^2} + \frac{\partial^2 w}{\partial y^2}\right).$$

Since the differential equation of a plate with unitormly distribnted load, q, is given by

$$\left(\frac{\partial^2}{\partial x^2} + \frac{\partial^2}{\partial y^2}\right)\left(\frac{\partial^2 w}{\partial x^2} + \frac{\partial^2 w}{\partial y^2}\right) = \frac{q}{D},$$

we get

$$\frac{\partial^2 M}{\partial x^2} + \frac{\partial^2 M}{\partial y^2} = -(1+\nu)q. \tag{1}$$

Applying polar coordinates for the above equation, we get

$$\frac{\partial^2 M}{\partial r^2} + \frac{1}{r}\frac{\partial M}{\partial r} + \frac{1}{r^2}\frac{\partial^2 M}{\partial \theta^2} = -(1+\nu)q. \tag{2}$$

As shown in Fig. 2, we divide the slab into two areas; the column portion and the middle portion. The former is the portion of the plate around a column, which is given as a circle with radius, a, i.e., half of the distance between two neighbouring columns and the latter is the portion of the plate surrounded by the boundaries of the other column portions.

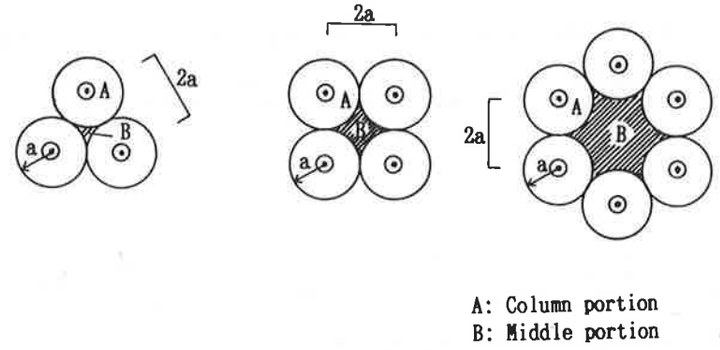

Fig. 2 Column portion and middle portion

The solutions for the column portion and the middle portion are denoted as M_1 and M_2, rerpectirely.

We utilize the analytical solution for a circnlar plate for the column portion.

Fig. 3(a) represents a circular plate of radius b (the radius of a column) with a load P concentrated at the center. The diflection of the plate at a distance r_1 from the center of the plate is provided by[3)]

$$w = -\frac{Pa^2}{8\pi D}\left\{(1+A)\left(1-\frac{r^2}{a^2}\right) - \left(B + \frac{r_1^2}{a^2}\right)\cdot\log\frac{a}{r_1}\right\} \tag{3}$$

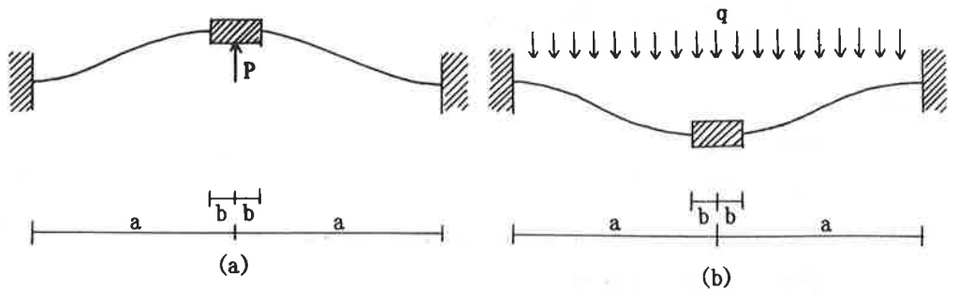

Fig. 3-(a) Circular plate with concentrated load
(b) Circular plate with uniformly distributed load

in which

$$A = \frac{b^2}{a^2 - b^2}\log\frac{a}{b} - \frac{1}{2}, \quad B = \frac{2b^2}{a^2 - b^2}\log\frac{a}{b}.$$

As shown in Fig. 3(b), the deflection of the plate with uniformly distributed load is

$$w = -\frac{qa^4}{64D}\left\{1 - \frac{r_1^4}{a^4} + 8(c+1)\left(1 - \frac{r^2}{a^2}\right)\left(\frac{b^2}{a^2}\right) + 4\left(E - 2\cdot\frac{b^2}{a^2}\cdot\frac{r_1^2}{a^2}\right)\cdot\log\frac{a}{r_1}\right\} \tag{4}$$

in which

$$C = -\frac{1}{4}\left(3 + \frac{a^2}{b^2}\right) + \frac{b^2}{a^2 - b^2}\cdot\log\frac{a}{b}, \quad E = \left(1 - \frac{4b^2}{a^2 - b^2}\cdot\log\frac{a}{b}\right)\cdot\frac{b^2}{a^2}$$

In the polar coordinates, M is expressed by[4)]

$$M = M_r + M_t = -D(1+\nu)\left(\frac{\mathrm{d}^2 w}{\mathrm{d}r^2} + \frac{1}{r}\frac{\mathrm{d}\omega}{\mathrm{d}r}\right) \tag{5}$$

Substituting Eqs. (3) and (4) into Eq. (5), the sum of the moments of the column portion, M_1, is obtained by

$$M_1 = -\frac{(1+\nu)}{2\pi}\cdot P\cdot\left(A + \log\frac{a}{r_1}\right) - \frac{(1+\nu)}{2}\cdot q\cdot\left\{b^2\left(C + \log\frac{a}{r_1}\right) + \frac{1}{2}r_1^2\right\}. \tag{6}$$

Now that M_1 has been obtained, we next consider the sum of the moments of the middle portion, M_2. The origin of coordinates is taken at the center of the middle portion ($r_2 = 0$) and the middle portion is of polygonal shape with sharp angles surrounded by the boundaries of the column portions ($r_1 = a$).

We find the solution $M_2 = 0$ around the boundaries of column portion and connect M_1 with M_2.

First of all we employ the following as one of the solution for M_2:

$$-\frac{1}{4}(1+\nu)qr_2^2,$$

which satisfies Eq. (2). Suppose the right hand side of Eq. (2) is equal to zero, we have Laplace's equation. Then we add either real or imaginary part of any complex function to the solution.

We choose the following complex function.

$$C_1 Z^n = C_1 r_2^n(\cos n\theta + i\sin n\theta) \qquad C_1\text{: const.}$$

of which the real part is

$$C_1 r_2^n \cos n\theta.$$

Furthermore, since a constant C_0 is also the solution for Eq. (1) with the right hand side equal to zero, we obtain

$$M_2 = C_0 - \frac{1}{4}(1+\nu)r_2^2 + C_1 r^n \cos n\theta$$

Letting

$$C_0 = \frac{1}{4}(1+\nu)qa'^2,$$

and substituting C_0 into the above equation for M_2, we get

$$M_2 = \frac{1}{8}(1+\nu)qa'^2\left\{2 - 2\left(\frac{r_2}{a'}\right)^2 + C_2\left(\frac{r_2}{a'}\right)^n\cdot\cos n\theta\right\} \tag{7}$$

with C_2 constant.

In the above equation, the line for $M_2 = 0$ presents a circle which a radius $r_2 = a'$ in counting only first two terws, while the line provides a polygonal with sharp angles in involving all the three terms.

(a) Rectangular arrangement

Since the area supported by a column is $4a^2$, the load P of this area is

$$P = 4qa^2.$$

Substituting P into Eq. (6) provides M_1.

Substituting $n = 4$ into Eq. (7), the line for $M_2 = 0$ forms a square with sharp angles. Determing C_2 by trial and error in such a way that it should correspond to the lines providing $r_1 = a$ for the column portion,

$$C_2 = 3/8.$$

We next determine a'. The radius of the circle, which touches internally the middle portion of the square shape with sharp angles, is $(\sqrt{2} = 1)a$.

Substituting $\theta = \pi/4$ (the horizontal axis is $\theta = 0$) and $M_2 = 0$ into Eq. (7) leads to

$$r_2 = 0.93a'.$$

Letting r_2 equal to the radius $(\sqrt{2} - 1)a$, we get

$$a' = \{(\sqrt{2} - 1)/0.93\}a.$$

The results are shown in Fig. 4. Outer lines give $M_2 = 0$, providing good agreement with four circles ($r_1 = a$). Inner curve, which is very similar to a circle, gives a half of $M_{2\max}$.

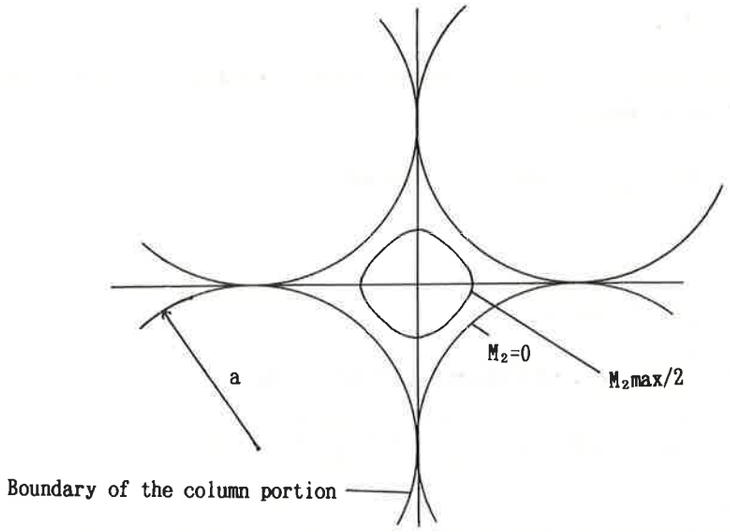

Fig. 4 Lines for $M_2 = 0$ and $M_{2\max}/2$ of middle portion

As an example, we calculate the case for $b = 0.2a$. In the column portion, we obtain from Eq. (6)

$$r_1 = b \quad M_1 = -5.22M_0 \quad M_0 = \frac{1}{8}(1 + \nu)qa^2$$

$$r_1 = a \quad M_1 = 1.31M_0.$$

At the center of the middle portion, we get from Eq. (7)

$$r_2 = 0, \quad M_2 = 0.40M_0.$$

Therefore, M at the center of the middle portion is

$$M = (1.31 + 0.40)M_0 = 1.71M_0.$$

Fourier series expansion technique provides the solution[5], $1.72M_0$. $1.71M_0$ is almost identrcal to the Fourier series solution. In obtaining the series solution, the column head shape is assumed to be a square. Transforming the sgnare to an equivalent circle, we find

$$K = 0.2/0.57 \times 2 = 0.175$$

In Fig. 5 M for each point between the column head and the center of the middle portion is depicted.

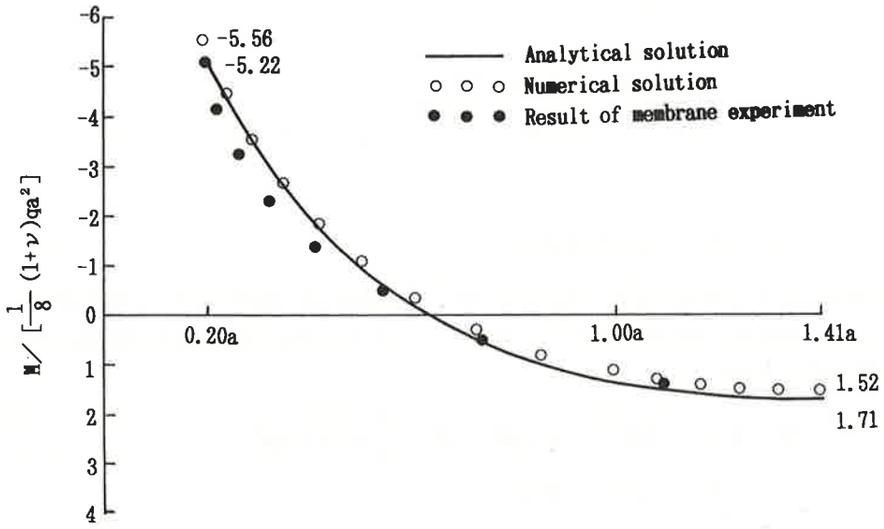

Fig. 5 Sum of bending moments (M) between column head and center of middle portion (Rectangular arrangement)

(b) Triangular arrangement

Substituting $P = 2\sqrt{3} \cdot qa^2$ into Eq. (6), we get M_1 in the column portion.

In order to get M_2, we substitute $n = 3$ into Eq. (7) and determine C_2 by trial and error, obtaining

$$C_2 = 3/4.$$

Substituting $\theta = \pi/3$ (the vertical axis is $\theta = 0$) and $M_2 = 0$ into Eq. (7),

$$r_2 = 0.87a'.$$

Sinre r_2 is equivalent to the radius of $(2/\sqrt{3} - 1)a$ of the inscribed circle, then

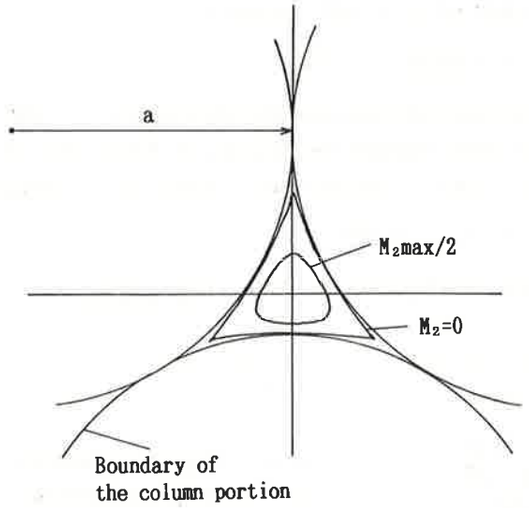

Fig. 6 Lines for $M_2 = 0$ and $M_{2\max}/2$ of middle portion

$$a' = \{(2/\sqrt{3} - 1)/0.87\}a.$$

As depicted in Fig. 6, the outer line is of $M = 0$, while the inner line is of half of $M_{2\max}$.

As an example, we calculate the case of $b = 0.2a$, which is same as the rectangular arrangement. Then,

$$M_1: \quad r = b \quad M_1 = -4.42M_0 \quad M_0 = \frac{1}{8}(1 + \nu)qa^2$$

$$r = a \quad M_1 = 1.02M_0$$

$$M_2: \quad r = 0 \quad M_2 = 0.06M_0.$$

At the center of the middle portion, M is

$$M = (1.02 + 0.06)M_0 = 1.08M_0.$$

In Fig. 7 M of each point on the line connecting the column head and the center of the middle portion is shown.

The ratio of the area supported by a column in this case to that in the rectangular arrangement is

$$2\sqrt{3}/4 = 0.866.$$

Letting the supporting areas for both arrangemcnts identical, M at the column is

$$-4.42/0.866 = -5.10.$$

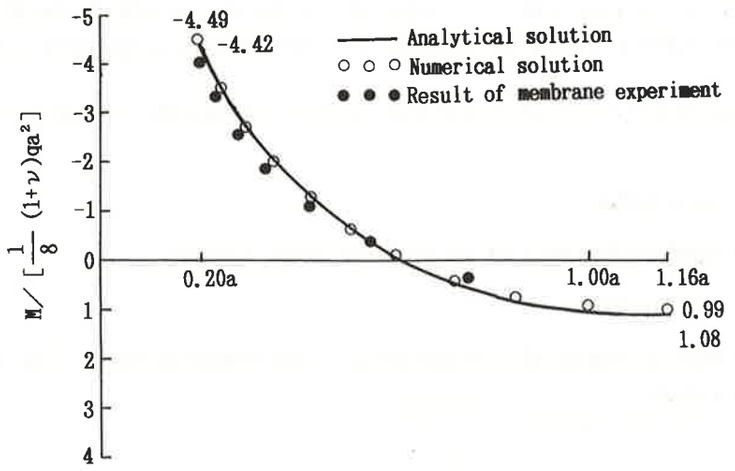

Fig. 7 Sum of bending moments (M) between column head and center of middle portion (Triangular arrangement)

It is quite close to -5.22 in the case of a rectangular arrangement. But, at the center of the middle portion, the sum of the bending moments decreases about 30%.

(c) Hexagonal arrangement

Substituting $P = 3\sqrt{3} \cdot qa^2$ into Eq. (6), and performing the same calculations, we obtain the result shown by a dashed line in Fig. 9. It is different from the value by other methodology, as will be explained later, because Eq. (6) has been obtained with the built-in boundary condition. The outer circular line of the column portion touches 6 other circles in a triangular arrangement, 4 in a rectangular arrangement, and only 3 in a hexagonal arrangement. It therefore seems that more circular plates around a column make the boundary condition closer to the built in.

For the hexagonal arrangement, the boundary of a column portion is assumed to have 1/2 of the bending moment for the radial direction with $r_1 = a$ substituted in Eq. (5). Both for concentrated and distributed loads, the ration of the bending moment for the radial direction to the bending moment for the tangential direction at the fixed end of a circular plate with clamped edges is

$$M_r{:}M_t = 1{:}\nu.$$

Estimating the bending moment at the boundary as

$$-\frac{1}{2(1 + \nu)} \cdot M_c,$$

in which M_c is provided with $r_1 = a$ substituted in Eq. (6), we add this bending moment value to the original solution given by Eq. (6) to get the bending moments in the column portion.

Substituting $\theta = \pi/6$ (the horizontal axis is $\theta = 0$) and $M_2 = 0$ into Eq. (7), we obtain

$$r_2 = 0.96a'.$$

Letting r_2 equal to the radius of the inscribed circle, we have

$$a' = a/0.96.$$

Two lines providing $M_2 = 0$ and $M_{2\max}/2$ are shown in Fig. 8. The latter looks similar to a circle.

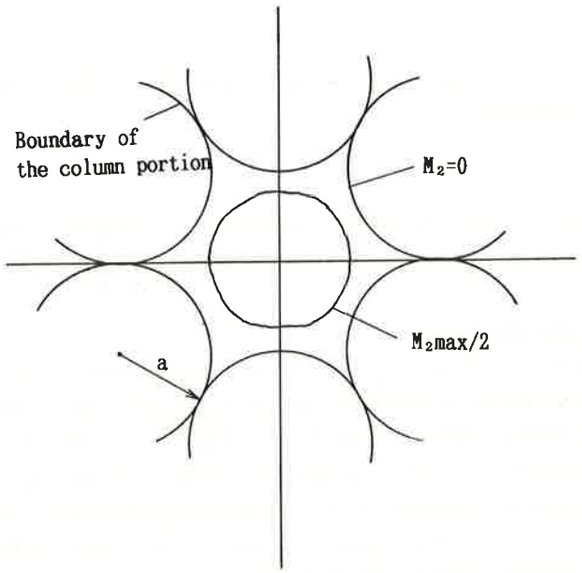

Fig. 8 Lines for $M_2 = 0$ and $M_{2\max}/2$ of middle portion

Taking the case of $b = 0.2a$ as an example, we get

$$M_C = 1.97M_0 \qquad -\frac{1}{2(1+\nu)}M_C = -0.82M_0 \quad (\nu = 0.2).$$

Adding this to Eq. (6) leads to

$$r_1 = b \quad M_1 = (-7.01 - 0.82)M_0 = -7.83M_0$$
$$r_1 = a \quad M_1 = (1.97 - 0.82)M_0 = 1.15M_0.$$

Substituting $r = 0$ into Eq. (7), we get

$$M_2 = 2.17M_1.$$

At the center of the middle portion,

$$M = (1.15 + 2.17)M_0 = 3.32M_0.$$

In Fig. 9 the solid line gives M on the line which connects the column head and the center of the middle portion. Dividing M by the ratio of areas supported by a column with hexagonal and square arrangements ($3\sqrt{3}/4 = 1.299$), it increases about 15% and 50% at the column head and at the center of the middle portion, respectively.

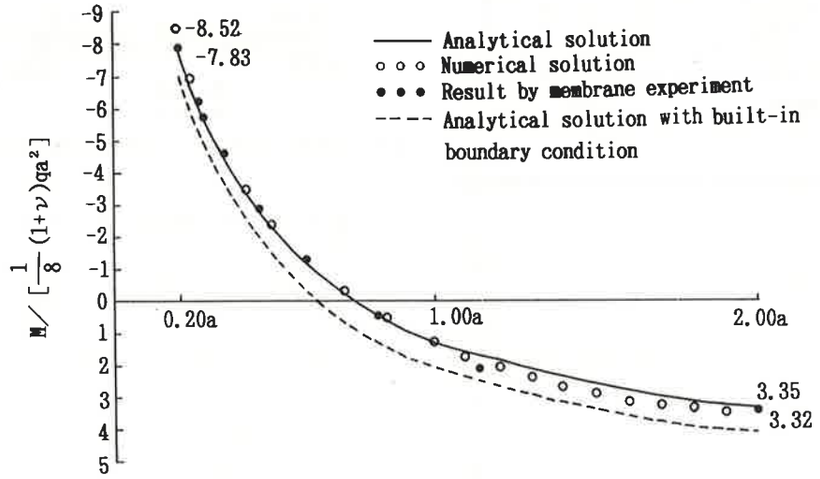

Fig. 9 Sum of bending moments (M) between column head and center of middle portion (Hexagonal arrangement)

1.2 Finite Element Analysis

Figures 10 ~ 19 are the finite element solutions for the bending moments of a plate. The finite element analyses are performed by the FEM program of FRAP-GEN, DEMOS.

In Figs. 5, 7, and 9 the white circles provide the sum of the bending moments, M, according to the F.E.M. In these figures the upper numerals indicate the finite element results, while the lower numerals the analyical solutions. They are in pretty good agreement.

On the line connecting two neighboring columns as shown in Figs. 11, 15 and 18, the bending moments with respect to the direstion parallel to the line, M_x, are identical for any column arrangement with the equal supporting area for one column. However, the bending moment with respect to the direction perpendicular to the line get larger in the order of triangular, rectangular and hexagonal arrangement.

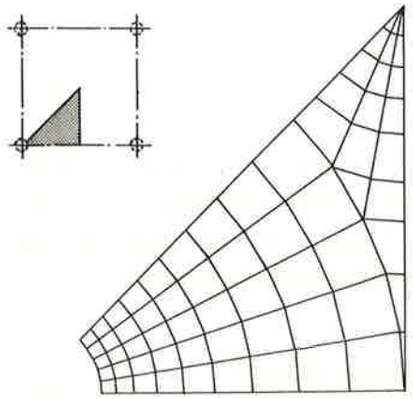

Fig. 10 Finite element model for rectangular arrangement

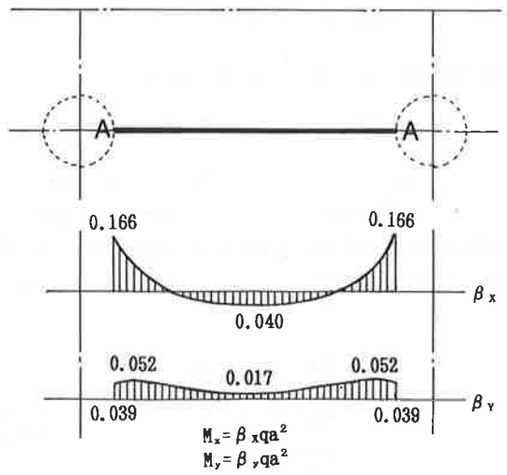

Fig. 11 Bending moments on column strip line ($\nu = 0.2$)

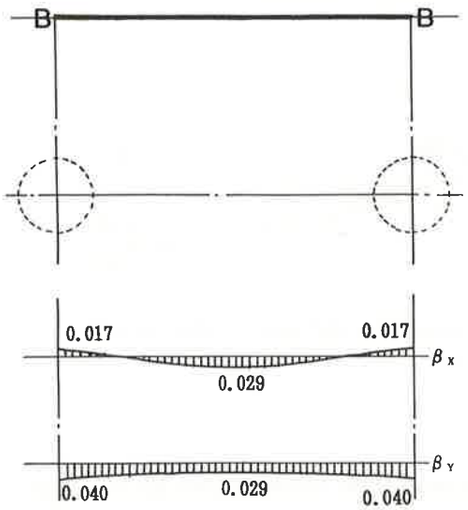

Fig. 12 Bending moments on center line of the slab

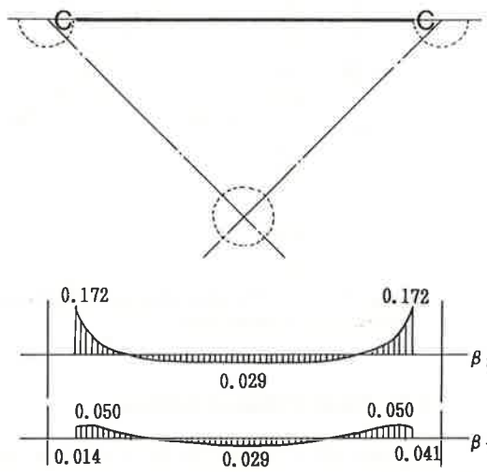

Fig. 13 Bending moments on diagonal

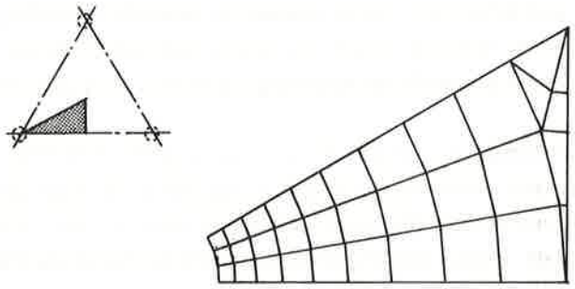

Fig. 14 Finite element model for triangular arrangement

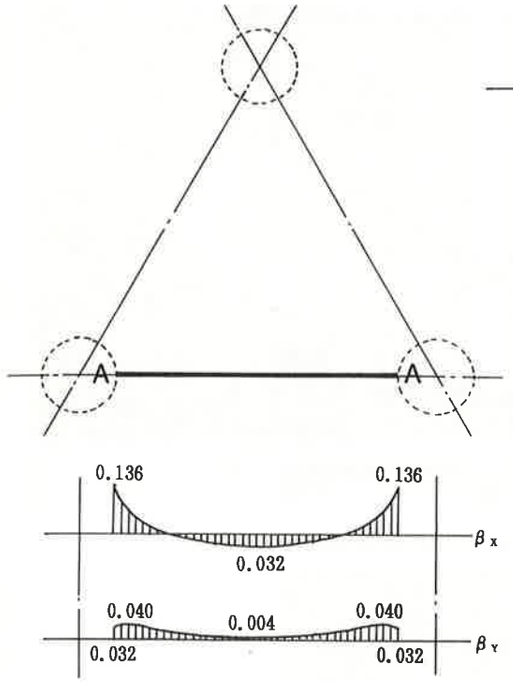

Fig. 15 Bending moments on column line

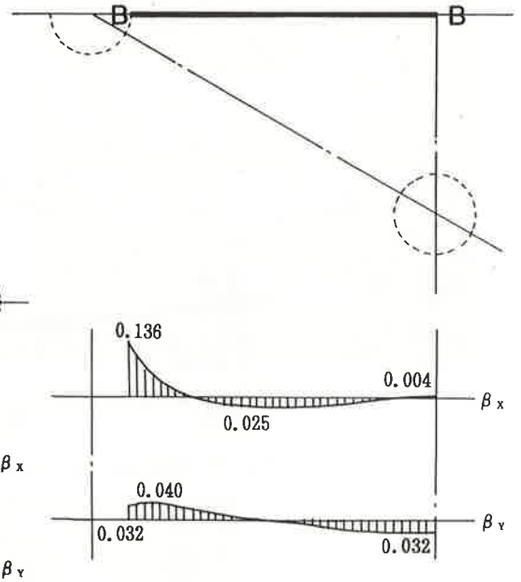

Fig. 16 Bending moments between column head and center of middle portion

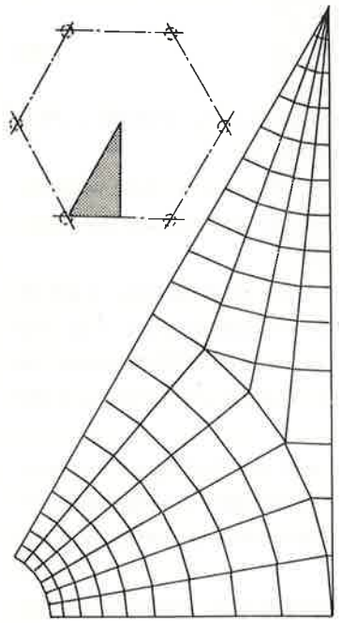

Fig. 17 Finite element model for hexagonal arrangement

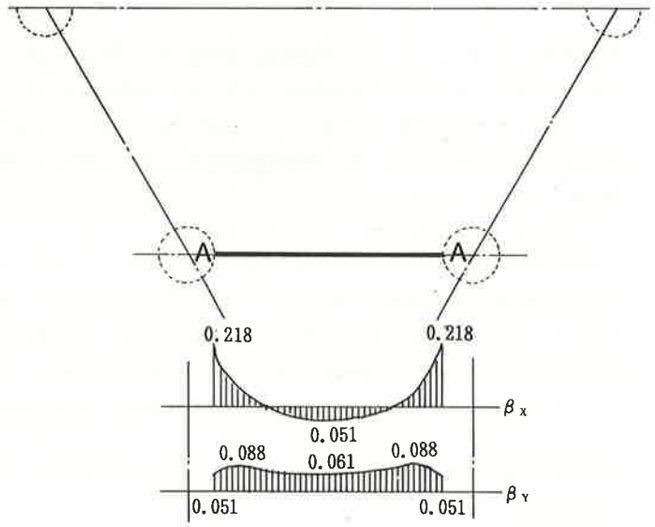

Fig. 18 Bending moments on column line

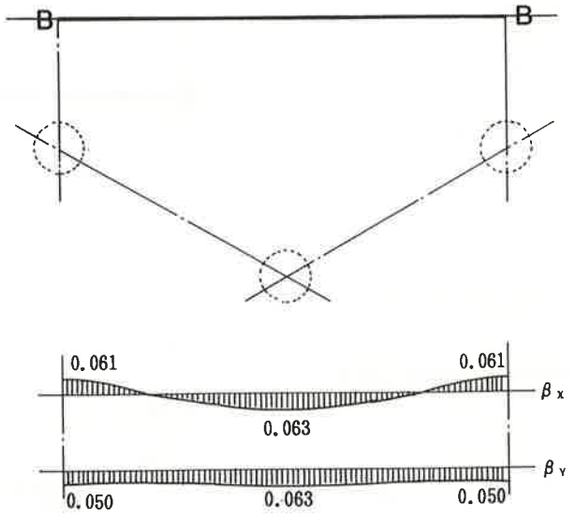

Fig. 19 Bending moments on center line of slab

1.3 Membrane Experiments

The deflection of a membrane, z, under a uniform load q and a uniform tension T is

$$\frac{\partial^2 z}{\partial x^2}+\frac{\partial^2 z}{\partial y^2}=-\frac{P}{T}. \tag{8}$$

Equation (8) provides the analogy to the equation of the sum of bending moments (M). Accordingly, we could measure M by the deflection of a membrane.

For the experiment, we apply uniform tension to a thin rubber membrane with the height of column equal to the height of the periphery of the frame, and provide the membrane with air pressure.

These experimental results are shown in Photos 1, 2 and 3. We establish the height of a contour line from membrane experiment with a simply supported square plate. The sum of the bending moments derived from the experiments are presented by black circles in Figs. 5, 7 and 9. They provide a good agreement with both the analytical solution and the finite element solution presented by the white circles.

Although a membrane experiment is easy to conduct and provides quite accurate results, it is difficult to decide the zero-order contour line. For the following examples, we obtain M at the column head from the analytical solution in similar way to the hexagon arrangement.

We show a combination of square and octagonal arrangements in Photo 4. We can recognize more contour lines at the octagonal portion. The value of M along the line connecting the column head and the center of the middle portion is given in Fig. 20. M is larger than in the case of a hexagonal arrangement with the equal supporting area.

Photo 1 Moire fringes of membrane experiment (Rectangular arrangement)

Photo 2 Moire fringes of membrane experiment (Triangular arrangement)

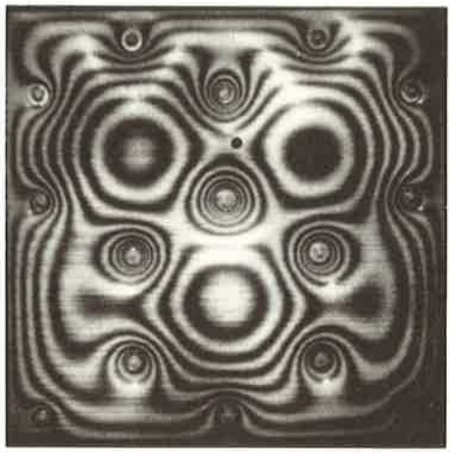

Photo 3 Moire fringes of membrane experiment (Hexagonal arrangement)

We get to the following concluding remarks:

1) Among three kinds of column arrangements, a triangular arrangement is a little more advantageous than a regular rectangular arrangement, and a hexaognal arrangement is the least advantageous.

2) Including the remarks(1), larger middle portion leads to less advantageous arrangement.

Photo 4 Moire fringes of membrane experiment (Combination of rectangular and octagonal arrangement)

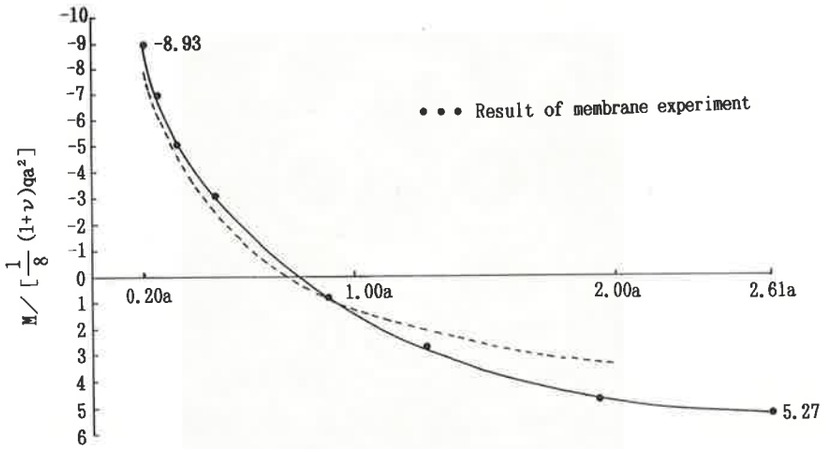

Fig. 20 Value of M (combination of regular rectangular and octagonal arrangement—dashed line refers to the hexagonal arrangement)

§2. SHEARING FORCES IN FLAT SLAB CONSTRUCTION

For flat slab construction, there have been many studies about the bending moments, but only a few theoretical studies about shearing forces have been reported. For a large amount of floor load or a large distance between two neighbouring columns, we have significant shearing forces around a drop panel. The distribution of the shearing forces depends on the shape of the drop panel.

In this section, we calculate the shearing forces of a plate for various shapes of the drop panel, utilizing the analogical relationship between the sum of the bending moments of a plate and the deflection of a membrane subjected to a distributed load.

2.1 Analogy between shearing forces of plate and deflections of membrane

The sum of bending moments of two perpendicular directions satisfies Eq. (1), which has exactly the same form as the equation of the membrane deflection provided by Eq. (8).

Denoting the magnitudes of shearing forces with respect to the x- and y-axes by Q_x and Q_y, respectively, and also denoting an arbitrary direction by n, we have

$$Q_n = Q_x \cdot \cos\alpha + Q_y \cdot \sin\alpha = -\frac{\partial}{\partial n}\left(\frac{\partial^2 w}{\partial x^2} + \frac{\partial^2 w}{\partial y^2}\right)$$

$$\therefore Q_n = \frac{1}{1+\nu}\frac{\partial M}{\partial n}. \tag{7}$$

where α is the angle between the x-axis and the n-direction.

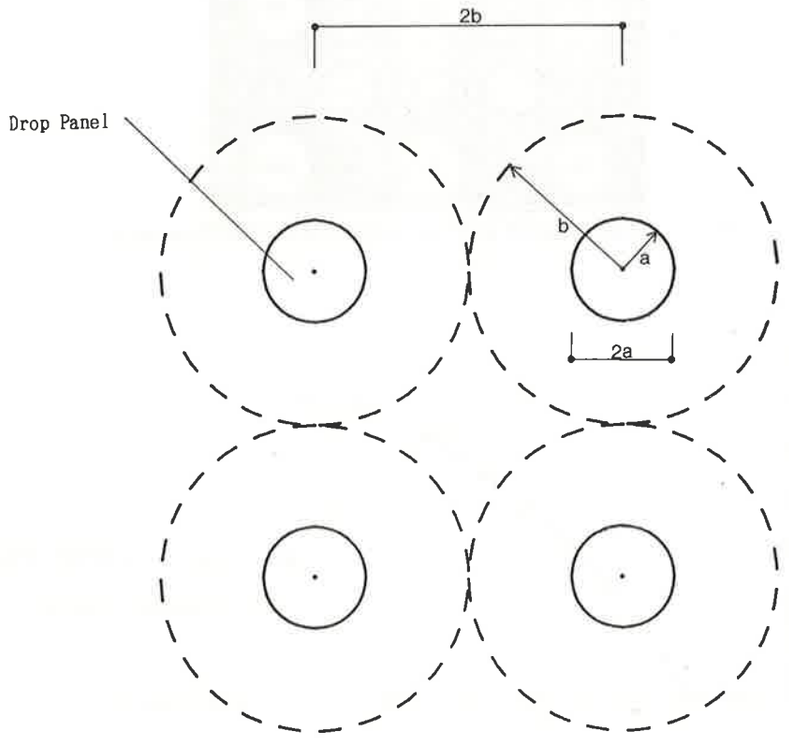

Fig. 21 Portions around columns

Since it is realized from Eq. (9) that differentiating the deflection of the membrane provides the shearing forces of a plate, the slope of the membrane corresponds to the shearing forces.

2.2 Sum of Bending Moments and Deflection of Membrane

1) Circular drop panel

We have a solution of Eq. (2) as follows:

$$M = -\frac{1+\nu}{4} qa^2 \left\{ 2\frac{b^2}{a^2} \cdot \log\left(\frac{a}{r}\right) + \left(\frac{r}{a}\right)^2 - 1 \right\}. \tag{10}$$

Letting $b = 2.5a$ in Eq. (10), the contour lines around the drop panel are found to form concentric circles as depicted in Photo 5.

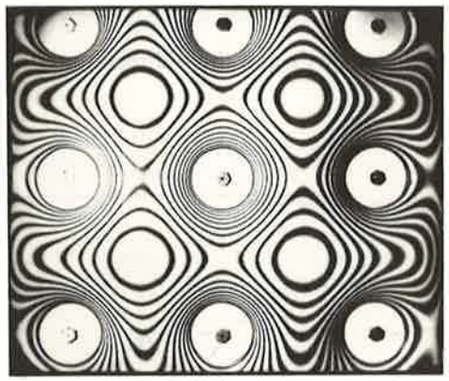

Photo 5 Moire fringes of membrane experiment (Circular drop panel)

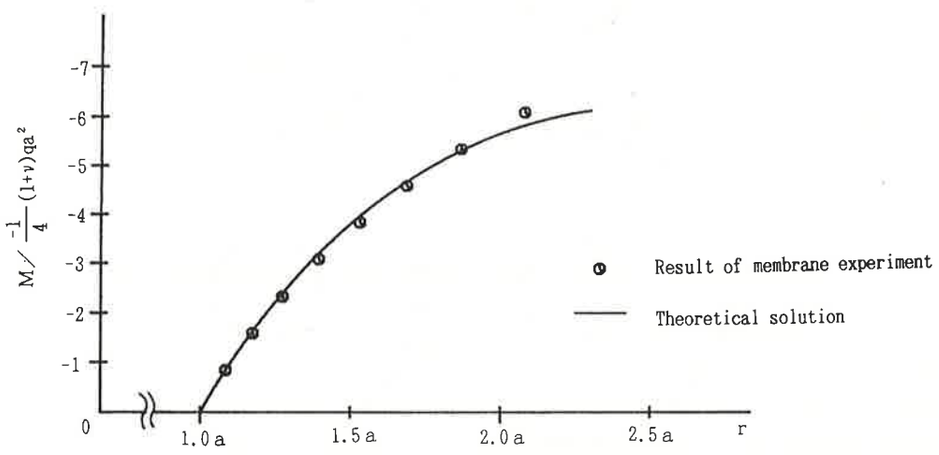

Fig. 22 Value of M for circular drop panel ($\theta = 0°$)

In Fig. 22 theoretical and experimental solutions are presented giving a good agreement.

2) Square drop panel with round angles

The following satisfies Eq. (5)

$$M = -\frac{1+L}{4} qa^2 \left\{ 2\frac{b^2}{a^2} \log\left(\frac{a}{r}\right) + \left(\frac{r}{a}\right) - 1 + \sum C_n \left(\frac{r}{a}\right)^{-n} \cdot \cos n\theta \right\} \tag{11}$$

$$C_4 = 3/4, \quad C_8 = 1/3, \quad C_{12} = 1/7$$

Making a use of this as a soultion leads to the fact that lines for $M = 0$ provide a kind of square shape with round corners. Photo 6 shows the contour lines of a similar square drop panel given by a membrane experiment. In Fig. 23 we find the theoretical and experimental solutions on the x axis close to each other. Good agreement between these solu-

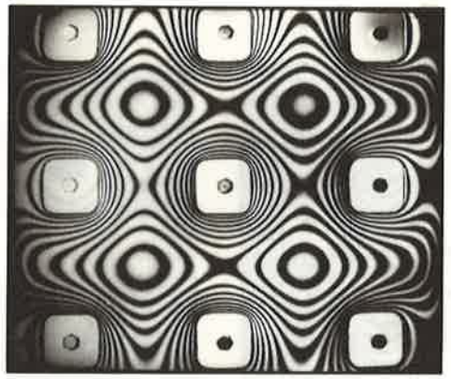

Photo 6 Moire fringes of membrane experiment (Square drop panel with round angles)

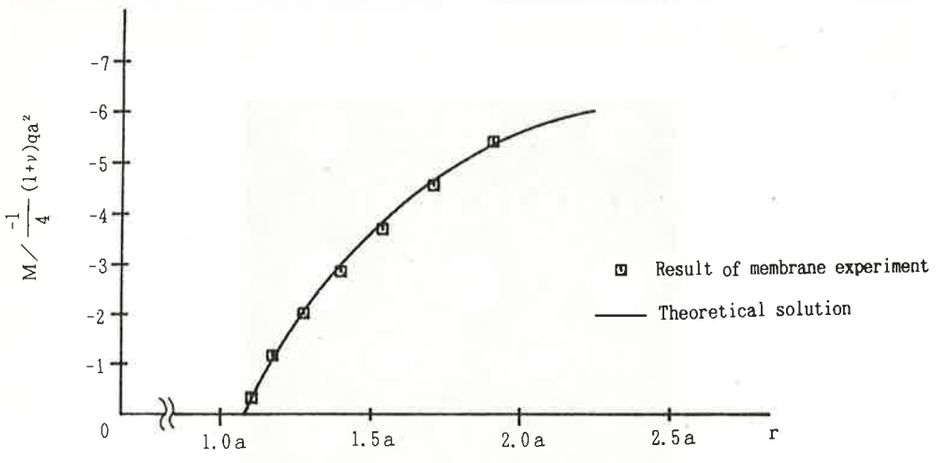

Fig. 23 Value of M (Square drop panel with round panel) ($\theta = 0°$)

tions indicates that the deflection of a membrane is well analogous to the sum of the bending moments.

3) Shearing forces and their maximums

Since differentiation of the sum of the bending moments leads to the shearing forces, we can obtain the shearing forces for several shapes of drop panels by measuring the slope of the membrane

$$Q_r = \frac{1}{1+\nu}\frac{\partial M}{\partial r}.$$

The shearing forces at the edge of a circular plate is used as a standard. Photos 7, 8 and 9 show the contour lines with square, hexagonal and octagonal panels. These lines becomes circles at a distance from a panel.

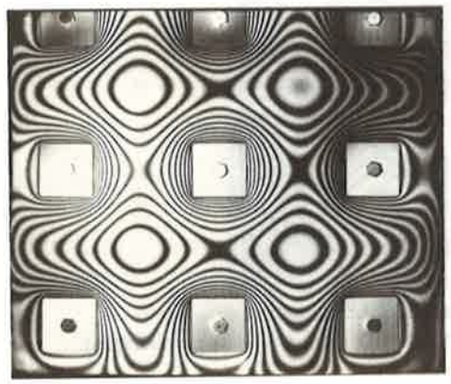

Photo 7 Moire fringes of membrane experiment (Square drop panel)

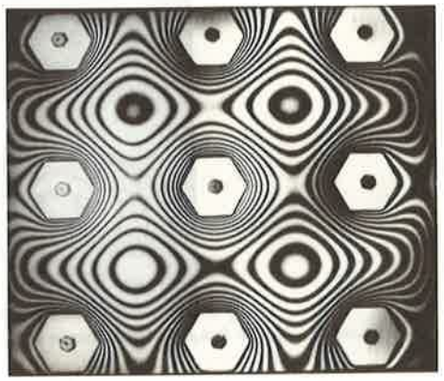

Photo 8 Moire fringes of membrane experiment (Hexagonal drop panel)

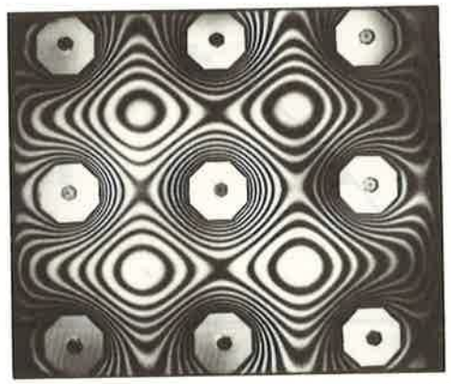

Photo 9 Moire fringes of membrane experiment (Octabonal drop panel)

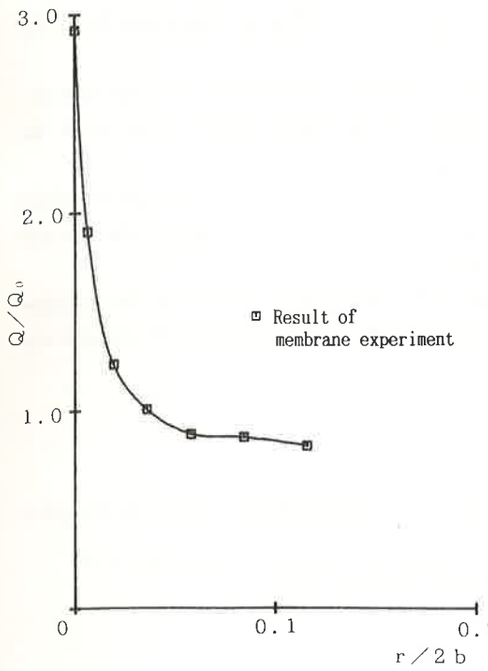

Fig. 24 Shearing forces for square drop panel ($\theta = 0°$)

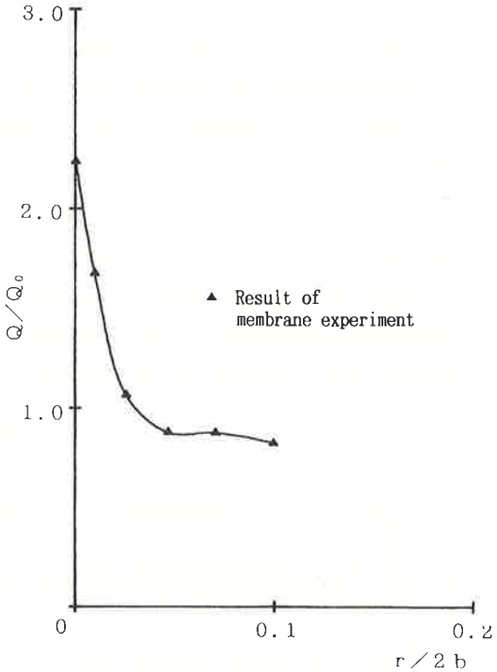

Fig. 25 Shearing forces for hexagonal drop panel ($\theta = 0°$)

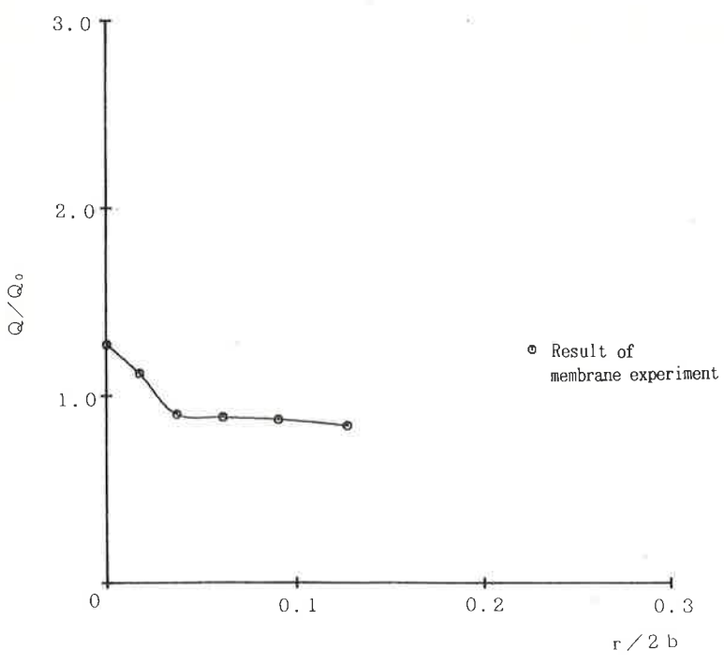

Fig. 26 Shearing forces for octagonal drop panel ($\theta = 0°$)

The shearing foroes are shown in Figs. 24, 25 and 26, which are obtained from the slope of the membrane in each corner.

In thses figues, the standard value is Q_0, wich is the shearing forces at the edge of a circular plate. The shearing forces are getting smaller for increasing the distance from the edge of panel.

The shearing force for a square is 2.9 times as large as for a circular panel, while those for a hexagonal and octagonal panels are 2.2 and 1.3 times, respectively. Square panel shape hence produces the maximum shearing forces.

From the above discussion concerning flat slab construction, we found that obtaining the shearing forces of a plate through the slope of a membrane is quite convenient and effective, and is expected to be very useful.

Refernces

1) Matsui, G. (1982), Structural Design in Flat Slab Construction, Monthly Building Engineering Magazine, Dec, pp. 88
2) Timoshenko, Woinowsky-Krieger. (1959), Theory of Plates and Shells, McGraw-Hill, pp. 81–92
3) JSME, Handbook for Mechanical Engineers 6th Edition, (1977), pp. 4–73
4) 2), pp. 52 Eq. (52)·(52)
5) 2), pp. 251
6) 2), pp. 56 Eq. (65), pp. 69 Eq(93)·(94)
7) 2), pp. 93
8) 2), pp. 81 Eq. (101)
9) 2), pp. 82 Eq. (103)
10) 29, pp. 82 Eq. (106)·(107)